

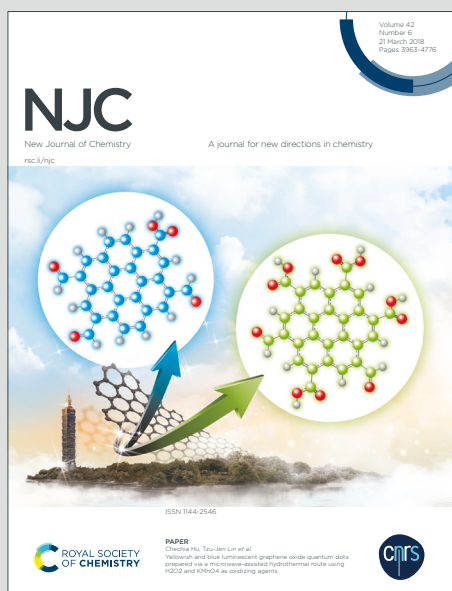
NJC

New Journal of Chemistry

Accepted Manuscript

A journal for new directions in chemistry

This article can be cited before page numbers have been issued, to do this please use: A. Marandi, M. Bahadori, S. Tangestaninejad, M. Moghadam, V. Mirkhani, I. Mohammadpoor-Baltork, R. Frohnhoven, S. Mathur, A. Sandleben and A. Klein, *New J. Chem.*, 2019, DOI: 10.1039/C9NJ02607J.



This is an Accepted Manuscript, which has been through the Royal Society of Chemistry peer review process and has been accepted for publication.

Accepted Manuscripts are published online shortly after acceptance, before technical editing, formatting and proof reading. Using this free service, authors can make their results available to the community, in citable form, before we publish the edited article. We will replace this Accepted Manuscript with the edited and formatted Advance Article as soon as it is available.

You can find more information about Accepted Manuscripts in the [Information for Authors](#).

Please note that technical editing may introduce minor changes to the text and/or graphics, which may alter content. The journal's standard [Terms & Conditions](#) and the [Ethical guidelines](#) still apply. In no event shall the Royal Society of Chemistry be held responsible for any errors or omissions in this Accepted Manuscript or any consequences arising from the use of any information it contains.

ARTICLE

Cycloaddition of CO₂ with epoxides and esterification reactions using the porous redox catalyst Co-POM@MIL-101(Cr)Received 00th January 20xx,
Accepted 00th January 20xx

DOI: 10.1039/x0xx00000x

Afsaneh Marandi,^a Mehrnaz Bahadori,^a Shahram Tangestaninejad,^{*a} Majid Moghadam,^{*a} Valiollah Mirkhani,^{*a} Iraj Mohammadpoor-Baltork,^a Robert Frohnhoven,^b Sanjay Mathur,^b Aaron Sandleben,^b Axel Klein.^b

The catalytic activity of the recently reported Co-POM@MIL-101(Cr) composite, synthesized from K₅[CoW₁₂O₄₀] (Co-POM) and chromium(III) terephthalate (MIL-101), was studied in the solvent-free cycloaddition of CO₂ with epoxides and esterification of acetic acid with various alcohols. The Co-POM@MIL-101(Cr) composite was synthesized using a one-pot HF-free method in a "bottle around ship" strategy. The material was thoroughly characterized using several methods such as (powder X-ray diffraction (PXRD), scanning electron microscopy (SEM), transmission electron microscopy (TEM), X-ray photoelectron spectroscopy (XPS), and electron paramagnetic resonance spectroscopy (EPR). Temperature programmed desorption (TPD) of NH₃ and CO₂, and the CO₂ adsorption capacity (adsorption isotherms) were used to study the acid-base properties of the materials. The combination of the electron-transfer character of Co(III)-POM and ordered mesopores in MIL-101(Cr) creates an efficient catalytic system with mild conditions (90 °C and 20 bar CO₂ pressure) for solvent-free cycloaddition of CO₂ to various epoxides. Esterification of acetic acid with alcohols was also carried out using the Co-POM@MIL-101 catalysts and high yields were achieved for different alcohols. The catalysis experiments also clearly show that the active site in this heterogeneous catalyst is the Co(III) center in the Keggin anion structure. It presumably conducts both the cycloaddition of CO₂ to epoxides and the esterification reaction *via* an outer-sphere electron transfer mechanism using the Co(III)/Co(II) redox pair. The heterogeneous Co-POM@MIL-101 catalysts were separated by simple filtration and reused five times in the cycloaddition of CO₂ with styrene epoxide and seven times for the esterification of acetic acid with benzyl alcohol with negligible leaching of Co-POM and no considerable loss of activity.

Introduction

Polyoxometalates (POMs) have attracted extensive attention in catalysis during recent years because of some unique characteristics such as fast reversible redox transformations under mild conditions and adjustable acid-base and redox properties in a wide range. To circumvent the POM's disadvantages such as low thermal stability, high solubility in water and polar media, and low surface area (1–10 m²g⁻¹), POM species have been supported on or encapsulated into suitable solid carriers with high surface area using strong dispersion forces.^{1–9} Among the various supports such as silica², titania³, activated carbon⁴, and zeolites⁵, metal-organic frameworks (MOFs) are very common, regarding their high capacity for catalyst loading and retention^{6–9}. The approach to encapsulate POMs in MOF cavities to provide heterogeneous catalysts has been reported before^{10–17} and their catalytic activity has been studied in important organic reactions such as

oxidations/epoxidations,^{11,14} hydrolysis of esters¹⁰, hydrolysis of epoxides,¹⁴ (trans)esterifications,^{10,16,17} or in the water splitting reaction.¹² The combination of POMs and MOFs should allow increasing stability, enhanced distribution of catalyst centers through large surface area, and easy separation from the reaction media.^{12,13}

The idea that reduction of POM acidity can be achieved through the interaction between the pores inner surface and POM through encapsulation¹⁸ inspired us to design a POM@MOF composite in which the POM acts as an electron transfer catalyst. For this reason, the Keggin anion [Co(III)W₁₂O₄₀]⁵⁻ polyoxometalate (Co-POM) with the ability of facile electron transfer through the redox couple Co(II)/Co(III)^{14,19–22} was chosen and its performance in heterogeneous catalytic reactions was investigated.

For the encapsulation of the Co-POM, the MOF should have large pores with small windows, capable of surrounding POMs and to prevent their leaching. Furthermore, the synthetic procedure for the MOF should not affect the properties of POM or lead to destruction of the structure. The large pores with pore windows smaller than Co-POM^{6,23} and the HF-free procedure for the synthesis of MOF²⁴ make MIL-101(Cr) suitable for this purpose. MIL-101(Cr) provides 29 and 34 Å mesoporous cages

^a Department of Chemistry, Catalysis Division, University of Isfahan, Isfahan 81746-73441, Iran

^b Department of Chemistry, University of Cologne, Greinstrasse 6, 50939 Köln, Germany

† E-mail addresses: stanges@sci.ui.ac.ir (S. Tangestaninejad), moghadamm@sci.ui.ac.ir (M. Moghadam), mirkhani@sci.ui.ac.ir (V. Mirkhani). ORCID: 0000-0001-5263-9795 (ST), 0000-0001-8984-1225 (MM), 0000-0003-0093-9619 (AK)

Electronic Supplementary Information (ESI†) available: [details of any supplementary information available should be included here]. See

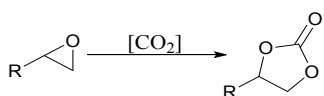
DOI: 10.1039/x0xx00000x

with free opening windows of 12 and 16 Å²⁵ and we consider encapsulation of Co-POM to be very efficient for this MOF.

In our previous report, a Co-POM@MIL-101(Cr) composite was synthesized and introduced as an electron transfer catalyst to carry out the ring opening reaction of epoxides with methanol.¹⁴ In this work, we focus on the encapsulation effect on the Co-POM activity and performance in the Co-POM@MIL-101(Cr) composite for the cycloaddition reaction of CO₂ with epoxides and for the esterification of acetic acid with various alcohols. The two different reactions were chosen to study a potential dual functionality of the MOF. In the esterification reaction, MIL-101 just acts as support for the Co-POM catalyst while in the cycloaddition reaction, MIL-101 captures CO₂ increasing its concentration around the catalytic species (Co-POM).

Catalytic "CO₂ fixation" into organic compounds for the production of commercially significant chemicals is one of the most promising approaches for CO₂ emission management simultaneously supplying an intermittent and renewable C1-feedstock.^{26,27} Among all introduced CO₂ transformation strategies, cycloaddition of CO₂ and epoxides to produce cyclic carbonates (Scheme 1) is one of the most promising routes, and significant progress has been made in recent years.²⁸⁻³⁰ Various advanced catalysts, both homogeneous and heterogeneous, have been developed in the past decade. Among currently available options, porous materials including porous carbon, porous silica and zeolites, porous organic polymers, and metal-organic frameworks (MOFs) are particularly attractive owing to their unique features such as large surface areas, high thermal stabilities, diverse building blocks, and ability to capture and storage of CO₂.³¹⁻³⁶ The high capacity of CO₂ adsorption and the presence of acidic or basic centers in this class of porous materials make them interesting materials for CO₂ capture and its catalytic conversion. At the same time, numerous examples of POM-based compounds have been reported as catalysts or promoters for CO₂ fixation processes.^{37,38}

The synergetic effect of POM and MOF as catalysts in the formation of cyclic carbonates from olefins was recently investigated by incorporating [ZnW₁₂O₄₀]⁶⁻ in a Zn-MOF structure.^{39,40}



Scheme 1. Cycloaddition of CO₂ and epoxide to a 1,3-dioxolan-2-one (cyclic carbonate).

The most common way to prepare an ester is the reaction of a carboxylic acid and an alcohol with the removal of water. This process is commonly carried out with base or acid catalysts.⁴¹⁻⁴³ Drawbacks of the such as severe conditions, noxious organic solvents, and exhaustive work-up can be circumvented by employing environmentally benign conditions and using heterogeneous acid catalysts.^{16,44,45} Assuming a lack of acidic character of the catalyst through the encapsulation,¹⁸ we wanted to test Co-POM@MIL-101 in the esterification of acetic acid to gauge if the encapsulation of the Co-POM catalyst can effectively prevent its Lewis acid-base interaction with the

substrate and instead trigger an electron-transfer mechanism for the esterification.

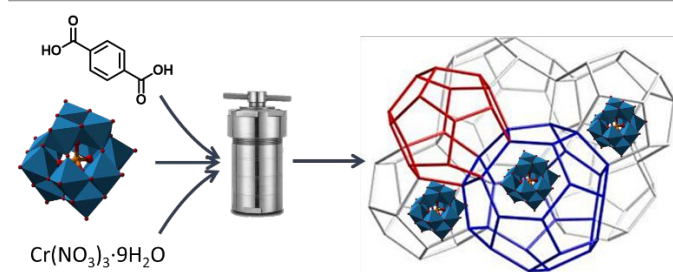
DOI: 10.1039/C9NJ02607J

The effect of several parameters including the amount of catalyst and temperature for both reactions, the pressure of carbon dioxide and reaction time for the conversion of CO₂ and the ratio of acid to alcohol for the esterification have been evaluated in this work alongside with a thorough characterization of the catalyst using powder X-ray diffraction (PXRD), scanning electron microscopy (SEM), transmission electron microscopy (TEM), X-ray photoelectron spectroscopy (XPS), and electron paramagnetic resonance spectroscopy (EPR).

Results and Discussion

Synthesis and characterization of the catalysts

Co-POM@MIL-101 composites containing varying amounts of Co-POM were prepared through the one-pot HF-free procedure reported previously (Fig. 1).¹⁴



name	initial amount of Co-POM
MIL-101(Cr)	-
Co-POM@MIL-101(1)	0.4 g (0.129 mmol)
Co-POM@MIL-101(2)	0.8 g (0.258 mmol)
Co-POM@MIL-101(3)	1.0 g (0.323 mmol)
Co-POM@MIL-101(4)	2.0 g (0.645 mmol)
Co-POM@MIL-101(5)	2.5 g (0.806 mmol)

Fig. 1. One-pot HF-free synthesis of Co-POM@MIL-101 composites.

The morphology of the Co-POM@MIL-101(3) composite was studied using TEM and SEM (Figures are shown in the Electronic Supporting Information ESI[†]). The images reveal micrometre-sized crystallites (Fig. S1) with sizes and shapes similar to those previously reported.¹⁴ Spherical interior particles show the incorporation of Co-POM into the MOF pores. The energy-dispersive X-ray spectroscopy (EDX) results obtained from SEM analysis clearly show the presence of Co and W from the Co-POM and Cr from the MIL-101(Cr) components (Fig. S2). The total amount of Co in Co-POM@MIL-101(3) is 0.1-0.2(1) wt%, the value for W of 27.9(2) wt% agrees roughly with a 7:1 ratio of MIL-101(Cr) and Co-POM. The elemental mapping analysis indicates a good distribution of Co-POM into the pores of MIL-101(Cr) (Fig. S2).

The X-band EPR spectrum of Co-POM@MIL-101(3) (Fig. 2, black trace) represents the typical isotropic, broad signal of MIL-101 containing Cr(III) (d³).⁴⁶ The spectrum of the Co-POM-rich Co-POM@MIL-101(5) (Fig. 2, red trace) seems to be composed of

the signal for MIL-101 with 8% of the original intensity and a further broad signal (see inset). We ascribe the loss of signal intensity for the second sample to oxidation of Cr(III) presumably to diamagnetic Cr(IV), while the broad featureless residual signal is probably due to Co(II) ions.⁴⁷⁻⁴⁹

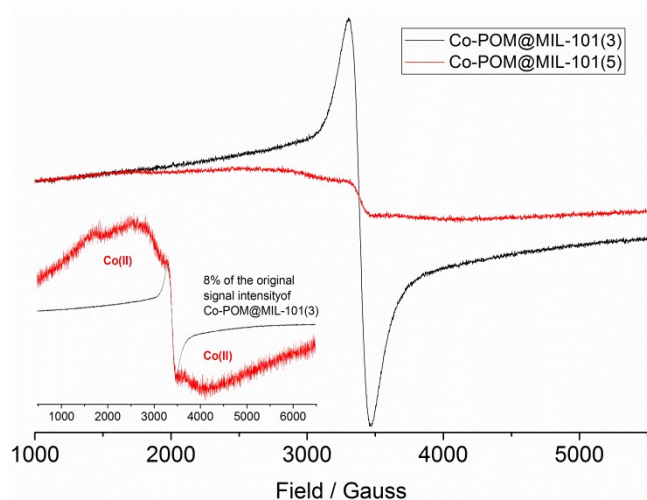


Fig. 2. X-band EPR spectra of Co-POM@MIL-101(3) (black) and Co-POM@MIL-101(5) (red) powder samples at 110 K, attenuation 25 dB, frequency. In inset shows that the signal of Co-POM@MIL-101(5) (red) is composed of 8% residual absorption of MIL-101 and signals presumably due to Co(II).

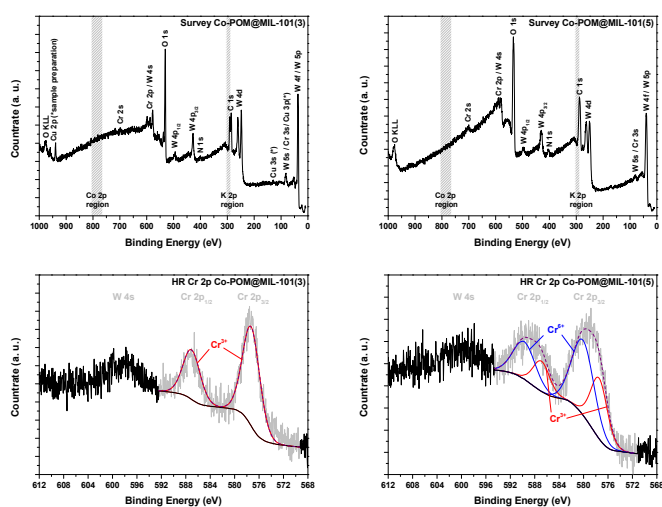


Fig. 3. XPS Survey Spectra for Co-POM@MIL-101(3) (top left) and (top right) Co-POM@MIL-101(5). XPS high-resolution spectra of the Cr 2p region for Co-POM@MIL-101(3) (bottom left) and Co-POM@MIL-101(5) (bottom right).

Co-POM@MIL-101(3) and Co-POM@MIL-101(5) were further investigated by X-ray photoelectron spectroscopy (XPS) regarding elemental composition and redox chemistry. XPS survey spectra (Fig. 3, top) for both samples show typical signals for C, O, N, Cr, and W, but neither for K nor for Co. Latter can be explained by the low Co content (far below 1 at%) in both samples in combination with the presence of large amounts of the heavy element W.⁵⁰ The absence of signals for K (in line with the EDX results) reveals the complete stripping of K⁺ ions during the synthesis of Co-POM@MIL-101 leaving back the Keggin

anion [CoW₁₂O₄₀]⁵⁻. Signals for Cu 2p, 3s, and 3p in the Co-POM@MIL-101(3) survey spectrum are caused by the Cu metal foil, which was used for sample preparation to avoid sample charging effects during measurement.

High-resolution Cr 2p spectra of both samples (Fig. 3, bottom) are in line with the results of EPR measurements. While in Co-POM@MIL-101(3) only one doublet is observed at 577.3 eV and 587.1 eV in good agreement with binding energies (BEs) for Cr(III) in Cr(OH)₃.⁵¹ The spectrum for Co-POM@MIL-101(5) exhibits next to the Cr(III) signal another doublet at 580.1 eV and 589.7 eV matching well with binding energies for Cr(IV) found in CrO₃,⁵¹ with a 62:38 ratio of Cr(IV) to Cr(III). Similar observations can be made in the high-resolution spectra of the W 4f / W 5p region (Fig. S3): Co-POM@MIL-101(3) shows only one doublet each, with binding energies of 35.6 eV and 37.8 eV for the W 4f doublet similar to W(IV) in WO₃,⁵² whereas Co-POM@MIL-101(5) features an additional doublet each, shifted to higher binding energies (38.6 eV and 40.8 eV). The intensity ratio here exhibits the same 62:38 ratio for the high binding energy doublet in comparison to the original W(IV) doublet as found for Cr(IV) to Cr(III). This goes along with the observation in the O 1s high-resolution spectra (Fig. S4) that the "lattice oxide" peak located at 530.7 eV, obviously attributed to the W-O bond in the Co-POM, decreases from Co-POM@MIL-101(3) to Co-POM@MIL-101(5), while the "defect oxide" component increases. Therefore, we suggest the high-BE species of W(IV) to be located at the oxidized Cr host matrix, which is promoted by oxidation of Cr(III) to Cr(IV) by the Co(III)/Co(II) redox pair.

A further interesting feature on the intrinsic CO₂ adsorption capability of MIL-101^{53,54} is revealed in the C 1s spectra (Fig. S5) of both samples. The as prepared measured sample Co-POM@MIL-101(3) shows a large signal at 291.7 eV in the C 1s spectrum accompanied by a pronounced signal at 538.1 eV in the O 1s spectrum (Fig. S4), both representing gaseous CO₂ molecules adsorbed in the pores of Co-POM@MIL-101.^{55,56} For the later measured, and therefore longer in vacuum stored Co-POM@MIL-101(5), these features are already strongly decreased.

The Lewis acidity and basicity of Co-POM, MIL-101(Cr), and Co-POM@MIL-101(3) were studied using temperature programmed desorption (TPD) experiments with ammonia (NH₃) and carbon dioxide (CO₂), respectively (Fig. 4). The acidity and basicity were determined from the peak area of the desorbed NH₃ and CO₂ (Table 1). Taking into account the thermal stability of Co-POM and MIL-101(Cr), 800 °C and 350 °C were chosen as the final temperatures for the data collection. The NH₃-TPD profile of Co-POM showed a desorption peak in the *T* range of 200 to 500 °C with a 280.4-339.2 μmol NH₃/g_{cat} ammonia adsorption capacity, which was attributed to weak/moderate acidic sites and a low intense desorption peak at higher *T* (500 to 800 °C) was referred to strong acidic sites (Fig. 4b). In view of the NH₃-TPD pattern for MIL-101(Cr), the acidity was classified into two groups: weak to medium (50 to 320 °C) and strong (320 to 350 °C) which is in accordance with recent work.⁵⁷ MIL-101(Cr) showed small desorption peaks in the weak-medium acid range with 1006 μmol/g_{cat} desorption capacity in line with low acidity. In the case of the strong acidity sites of MIL-101(Cr),

it is difficult to determine the accurate amount of desorption capacity due to decomposition of MIL-101(Cr). For the Co-POM@MIL-101(3) composite, the origin of this peak can be either MIL-101 or Co-POM.

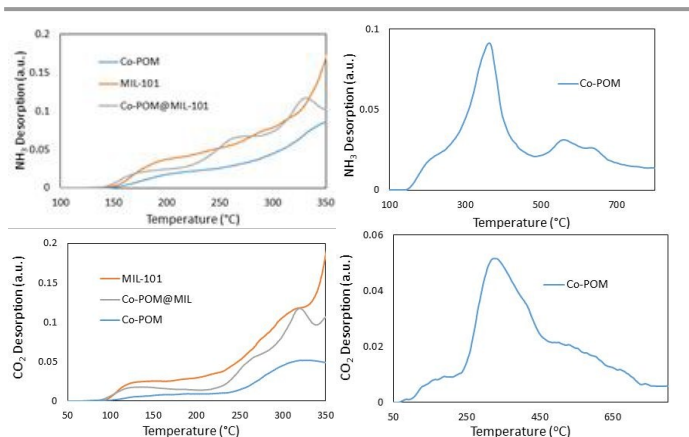


Fig. 4. Temperature programmed NH₃ and CO₂ desorption (TPD) profiles of Co-POM, MIL-101(Cr), Co-POM@MIL-101(3).

Fig. 4c and 4d shows the CO₂-TPD profiles of the Co-POM@MIL-101(3) composite, Co-POM, and MIL-101(Cr) and corresponding numerical values of the integrated desorption peaks were obtained 1109.5, 522, and 1485 μmol CO₂/g_{cat}, respectively (Table 1). The observed basicity was attributed the terephthalate O atoms in the MOF or to O atoms in the WO₆ clusters in POM structure.^{57,58} However, the thermal stability of MOFs should be taken into full account during examination. Due to the existence of organic ligands, the degradation of MOFs can also yield CO₂ in most cases. It is unlikely to distinguish the CO₂ desorbed from basic sites and the CO₂ from MOFs⁵⁹ degradation that this phenomenon can be observed in the CO₂-TPD profile of MIL-101 and composite catalyst (Fig. 4).

The N₂ adsorption in BET (Brunauer–Emmett–Teller) experiments at 77 K (Fig. 5) showed two uptakes at $P/P_0 = 0-0.15$ and $P/P_0 = 0.15-0.22$ resulting from two kinds of nanoporous windows. For the Co-PO@MIL-101(3) sample the uptake volume is markedly decreased compared with MIL-101 in line with the encapsulation of the Co-POM. Also, N₂ adsorption-desorption for MIL-101(Cr) and Co-POM@MIL-101 with different Co-POM loading revealed a decrease in nitrogen adsorption (Fig. S6 in the ESI†). The pore size distribution

curves were calculated using the Barrett, Joyner, and Halenda (BJH) equation. The pore size distribution curve of Co-POM@MIL-101(3) is in good agreement in comparison with pure MIL-101(Cr). However, the decrease of total pore volume in the composite catalyst confirming that the Co-POM species were successfully encapsulated to the inner pores of MIL-101(Cr) framework. Nevertheless, the free pore space preserved after encapsulation was sufficient for the efficient transfer of substrate molecules for catalysis as shown later.

To demonstrate the potential of the Co-POM@MIL-101 composites for CO₂ gas absorption (Fig. S7 in the ESI†), we measured the adsorption isotherms of CO₂ at 0 °C after evacuation of the samples at 100 °C for 12 h. As expected, the CO₂-adsorption capacity of composite catalyst is lower than pure MIL-101(Cr), because of the presence of Co-POM in the pore of MIL-101.

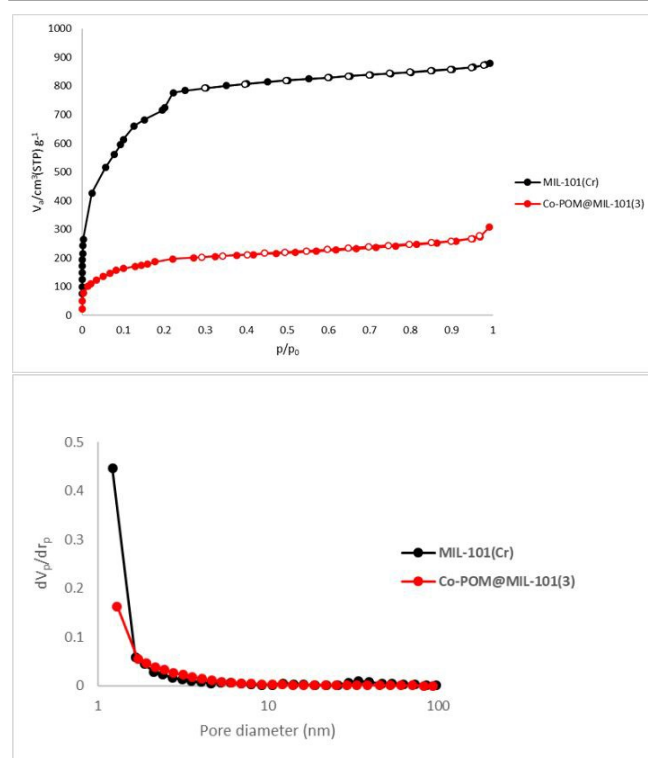


Fig. 5. N₂ adsorption-desorption isotherms (top) and BJH plot (bottom) for MIL-101(Cr) and Co-POM@MIL-101(3)

Table 1. Results from temperature programmed desorption (TPD) measurements for NH₃ and CO₂

sample	total NH ₃ μmol/g catalyst	NH ₃ -TPD			total CO ₂ μmol/g catalyst	CO ₂ -TPD		
		weak acid	medium	strong acid		weak base	medium	strong base
Co-POM	1372 ^a	222.1	709.7	439.69	522	43.7	339.1	138.7
MIL-101(Cr)	1463.5 ^b	1006	-	458.1	1485	218	-	1269.4
Co-POM@MIL-101(3)	1278 ^b	884.1	-	394.47	1109.5	144	-	965.6

^a 96-800 °C. ^b 98-350 °C

ARTICLE

Table 2. Results of the ICP and BET analysis for Co-POM@MIL-101 with varying amounts of Co-POM.

sample	Co-POM (g)	amount of loaded POM ^a (mmol/g)	BET surface area (m ² /g)	average pore diameter (nm)	total pore volume (cm ³ /g)
MIL-101	0	-	2564	2.36	1.5
Co-POM@MIL-101(1)	0.4	0.0050	1842	2.6	0.82
Co-POM@MIL-101(2)	0.8	0.0084	988	2.0	0.50
Co-POM@MIL-101(3)	1	0.0100	683	1.8	0.47
Co-POM@MIL-101(4)	2	0.0130	545	1.7	0.33

^aDetermined by ICP.**Cycloaddition of CO₂ with epoxides**

The Co-POM@MIL-101 catalysts were used for the cycloaddition of styrene oxide as a model reaction at 110 °C under 20 bar CO₂ pressure and solvent-free conditions using tetra-*n*-butylammonium bromide (TBABr) as co-catalyst for this reaction (Table 3). TBABr is used in this reaction for activation of the reactants opening the epoxide ring through nucleophilic attack and form a bromo-alkoxide and also an active CO₂ molecule.⁶⁰ As expected, the conversion increases with increasing Co-POM loading from 0.4 to 1.0 g. However, also MIL-101(Cr) catalyses the reaction, although with somewhat poorer performance. A further increase of Co-POM to 2.0 g resulted in a reduction in both conversion and selectivity. This is in line with the ICP analysis (Table 2) confirming a larger loading for Co-POM@MIL-101(4) with 0.0130 mmol/g encapsulated Co-POM reducing the specific surface area and total pore volume.

On the other hand, the surface area is affected by both initial and loaded Co-POM. Increasing the initial Co-POM reduces the crystallinity of the structure of MOF and subsequently the surface area. Considering all factors including the specific surface area of the MIL-101 support, loading of Co-POM, and the results from Table 3, Co-POM@MIL-101(3) with 0.0100 mmol/g encapsulated Co-POM was chosen as the optimized catalyst loading for further reactions.

Table 3. The effect of the initial POM amount in the catalytic activity of the Co-POM@MIL-101 catalysts in the cycloaddition of CO₂ with styrene epoxide a

sample	Co-POM (g)	conversion (%) ^b	selectivity (%) ^b
MIL-101(Cr)	0	66	83
Co-POM@MIL-101(1)	0.4	68	84
Co-POM@MIL-101(2)	0.8	73	88
Co-POM@MIL-101(3)	1	88	88
Co-POM@MIL-101(4)	2	69	85

^a Reaction conditions: 15 mmol styrene epoxide, 200 mg catalyst, 1 mmol TBABr, *P*_{CO₂} = 20 bar, *T* = 110 °C, 2 h.

The cycloaddition of styrene epoxide with CO₂ without the catalyst performed as a control reaction at 110 °C under solvent-free conditions and 20 bar CO₂ pressure afforded no product, proving that the catalyst is necessary (Table 4, entry 1). Also, the yield of the reaction was negligible when the catalyst was used without co-catalyst (entry 3).

Table 4: Cycloaddition of CO₂ with styrene epoxide a

entry	catalyst	conversion (%) ^b	selectivity (%) ^b
1	-	0	0
2	Co-POM ^c	negligible	negligible
3	Co-POM@MIL-101(3)	18	55
4	TBABr ^d	49	82
5	Co-POM/TBABr ^e	53	76
6	MIL-101/TBABr	66	83
7	Co-POM@MIL-101(3)/TBABr	88	88

^a Reaction conditions: 15 mmol styrene epoxide, 200 mg catalyst, 1 mmol TBABr, $P_{\text{CO}_2} = 20$ bar, $T = 110$ °C, 2 h. ^b Yields were determined by GC analysis. ^c Reaction conditions: 15 mmol styrene epoxide, 10 mg Co-POM, $P_{\text{CO}_2} = 20$ bar, $T = 110$ °C, 2 h. ^d Reaction conditions: 15 mmol styrene epoxide, 1 mmol TBABr, $P_{\text{CO}_2} = 20$ bar, $T = 110$ °C, 2 h. ^e Reaction conditions: 15 mmol styrene epoxide, 10 mg Co-POM, 1 mmol TBABr, $P_{\text{CO}_2} = 20$ bar, $T = 110$ °C, 2 h.

Furthermore, the effects of reaction temperature, CO₂ pressure, reaction time and amount of the catalyst were investigated. The reactions of styrene oxide (15 mmol) in the presence of TBABr (1 mmol) and catalyst (200 mg) under pressure of CO₂ (20 bar) and 110 °C at various reaction times (1 to 5 h) were checked and 2 h was selected for the reaction time based TOF (h⁻¹) (Table S1 in the ESI⁺). Also, the effect of reaction temperature was studied in detail (Table S2). The results showed good conversion at 90 and 110 °C, while lower conversion and selectivity was observed at 70 and 130 °C. While at 70 °C the catalyst might not be active, at 130 °C the decrease of the CO₂ solubility in the liquid phase might play a role. When exploring the effect of the catalyst amount on conversion and selectivity under the optimized conditions, 90 °C, 20 bar CO₂ pressure and 15 mmol styrene oxide under solvent-free conditions (Table S3) the conversion and selectivity was excellent at 200 mg catalyst load.

A detailed look at conversion and selectivity (Fig. 6) revealed that they both increased in the range of 10 to 20 bar of CO₂ pressure, but rising the pressure to 25 bar led to a slight decrease in both conversion and selectivity. As expected, increasing the solubility of CO₂ in the liquid phase by increasing the pressure results in the rise of both selectivity and conversion. An alternative explanation is the formation of an CO₂-epoxide "complex" intermediate at higher pressure overruling the catalyst-epoxide interaction.⁶¹⁻⁶³ A combination of the two opposite factors might be responsible for the enhancement of selectivity and conversion up to 20 bar and the reduction at a higher pressure of 22 and 25 bar (Fig. 6).

Finally, 20 bar CO₂ pressure, 90 °C temperature, 2 h reaction time, 15 mmol epoxide, 1 mmol TBABr and 200 mg Co-POM@MIL-101(3) under solvent-free conditions were selected as optimized conditions for the reaction of various

epoxides with CO₂ (Table 5). The results show excellent conversion and selectivity for all substrates. The best conversion was achieved for 1,2-epoxyhexane and epichlorohydrin (Table 5, entries 1 and 4). The reactivity of 1,2-epoxy-3-phenoxypropane was relatively lower than the other substrates (Table 5 entry 6). Also, cyclohexane oxide as non-terminal epoxide presented excellent conversion and good selectivity (Table 5 entry 8) while poor reactivity has been previously reported for this epoxide.^{64,65}

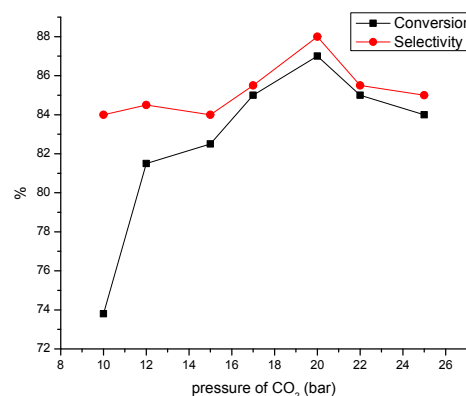
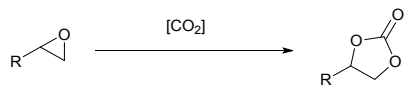
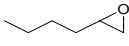
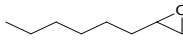
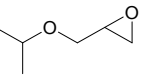
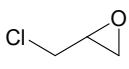
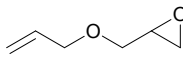
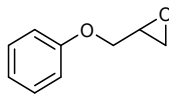
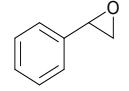


Fig. 6. Conversion and selectivity of styrene epoxide to cyclic carbonate as a function of pressure (bar) at 90 °C using 15 mmol styrene epoxide, 200 mg Co-POM@MIL-101(3) after 2 h.

The mechanism of the cycloaddition of CO₂ with epoxides using Co-POM@MIL-101(3) is proposed based on previous reports.^{38,66,67} Various research suggested a Lewis acid mechanism for the Co(III)-catalyzed cycloaddition of CO₂ with epoxides,⁶⁸ which cannot be considered for Co-POM@MIL-101(3) because of the shielding of the cobalt center with 12 WO₆ ligands. Alternatively, single-electron transfer from epoxide to cobalt(III) can occur³⁸ which produces oxygen radicals and carbon cations as intermediates as well as Co(II)-POM (Scheme 2). Nucleophilic attack of CO₂ followed by electron transfer from Co(II) to the intermediate forms the cyclic carbonate and recovers Co(III)-POM. In order to confirm the proposed mechanism, a model reaction (5 mmol acetic acid, 55 mmol benzyl alcohol, Co-POM@MIL-101(3), $T = 100$ °C) was carried out in the presence of acrylonitrile and 2,6-di-tert-butylphenol as radical scavengers. The yield of the product was significantly reduced under these conditions. This mechanism is also in line with the observed tendency of Co-POM@MIL-101 to undergo electron transfer from Cr(III) to Co(III) forming Co(II) (see EPR and XPS).

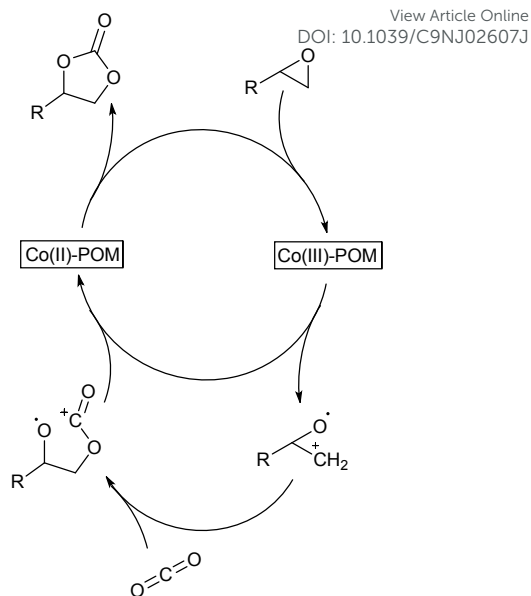
Table 5: Cycloaddition of CO₂ with various epoxides catalyzed by Co-POM@MIL-101(3)^a


entry	epoxide	conversion (%) ^b	selectivity (%) ^b
1		93	91
2		90	95
3		89	74
4		94	92
5		92	95
6		81	90
7		88	88
8		87	65

^a Reaction conditions: 200 mg catalyst, 15 mmol epoxide, P_{CO_2} = 20 bar, T = 90 °C, 2 h. ^b Yields were determined by GC analysis.

Esterification of acetic acid with alcohols

The esterification of acetic acid with various alcohols including different derivatives of benzyl alcohol and aliphatic alcohols such as 2-phenyl-1-propanol, 2-phenylethanol was studied in the presence of the catalysts Co-POM@MIL-101(3). The molar ratio of acid to alcohol was found to be the most significant factor, hence this effect was investigated by changing the molar ratio from 1:5 to 1:14 (Table 6). Other conditions including the reaction temperature (100 °C) and amount of the catalyst (100 mg) were held constant. The conversion increased significantly with increasing acid to alcohol molar ratio from 1:5 to 1:11.

**Scheme 2.** Proposed mechanism for cycloaddition of CO₂ with epoxides catalyzed by Co-POM@MIL-101(3).

As the esterification reaction is reversible; an excessive amount of alcohol is beneficial for the yield of the ester products. However, too much alcohol was unfavorable because of dilution of the catalyst and acetic acid.⁶⁹ Thus, a molar ratio of 1:11 acid:alcohol was chosen for further studies.

Table 6. Effect of acid to alcohol molar ratio ^a

entry	acid to alcohol ratio	yield (%) ^b
1	1:5	68
2	1:8	75
3	1:11	84
4	1:14	84

^a Reaction conditions: 5 mmol acetic acid, benzyl alcohol, 100 mg Co-POM@MIL-101(3), T = 100 °C, 25 min. ^b GC yield based on acid.

For the selection of the best catalyst with respect to Co-POM loading, esterification of acetic acid with benzyl alcohol with a molar ratio of 1:11 was performed at 100 °C using 100 mg Co-POM@MIL-101 with different amounts of Co-POM (Table S4). The results show the best TOF for Co-POM@MIL-101(3) with 0.01 mmol/g of POM loading. Optimization of the amount of Co-POM@MIL-101(3), based on the TOF (h^{-1}), was carried out using various amounts of the catalyst (50, 100 and 150 mg). The most efficient conversion was obtained in the presence of 100 mg catalyst (containing 0.0010 mmol Co, Table S5). For the exploration of the effect of reaction temperature on the yield, four experiments were performed at room temperature, 50, 70 and 100 °C (Table S6), and 70 °C was chosen as the optimum reaction temperature.

ARTICLE

New J. Chem.

The progress of the reaction was monitored by GC and the results are shown in Table 7. As can be seen, benzyl alcohols with electron donating groups are more reactive than those with electron withdrawing groups (entries 2-5). It is also noteworthy that aliphatic alcohols such as 2-phenyl-1-propanol and 2-phenylethanol (entries 6 and 7) were also converted to their corresponding esters in high yields. The turnover frequencies (TOF), mole of produced acetate ester per mole of Co-POM per hour range from about 7000 to 13000.

From the TPD experiments (Table 1) we have learned that MIL-101(Cr) has higher acidity compared with Co-POM while the results in Table S4 (in the ESI) show no activity of MIL-101(Cr) in the esterification reaction, while Co-POM@MIL-101 is a good catalyst. It is thus reasonable to assume that the catalytic activity of Co-POM@MIL-101 is not related to its acid-base properties. As said before the Co center is embedded within the lacunar Keggin anion and thus hampered from acid-base interaction with the substrate.^{70,71} Therefore, an outer-sphere electron transfer is possibly triggering the esterification mechanism as has been shown before for [CoW₁₂O₄₀]⁵⁻ in other reactions.¹⁹⁻²²

Using acrylonitrile and 2,6-di-tert-butylphenol as a radical scavenger in a model reaction (5 mmol acetic acid, 55 mmol benzyl alcohol, Co-POM@MIL-101(3), T = 100 °C) resulted in the reduction of the conversion from 84% to less than 20% confirming the presence of radical intermediates in the esterification reaction.

When compared to related MOF/POM based heterogeneous catalysts (Table 8), the Co-POM@MIL-101 system combines very low reaction times, solvent-less reactions, high reusability and low reaction temperature with high selectivity and TOF in this esterification reaction.

Reusability of the catalysts

In order to investigate the reusability of the catalyst Co-POM@MIL-101(3) and exclude that leached homogeneous catalytic species play a role in the esterification reaction, activated catalyst and benzyl alcohol were reacted for 1 h (conditions as in Table 6), then the catalyst was separated by filtration. In the next step, acetic acid was added to the reaction vessel and the reaction mixture was stirred again. The reaction progress was followed by GC and no noticeable conversion was observed. To study the stability and reusability of Co-POM@MIL-101 catalyst in the cycloaddition of epoxide with CO₂, five reaction cycles were carried out using styrene epoxide in a model reaction (Fig. 7). After each run, the catalyst was filtered off, washed with ethyl acetate and activated in a vacuum oven at 100 °C for 24 h to remove trapped reactants. Also, seven cycles of esterification reaction were carried out using acetic acid and benzyl alcohol in a model reaction (Fig. 8).

View Article Online

DOI: 10.1039/C9NJ02607J

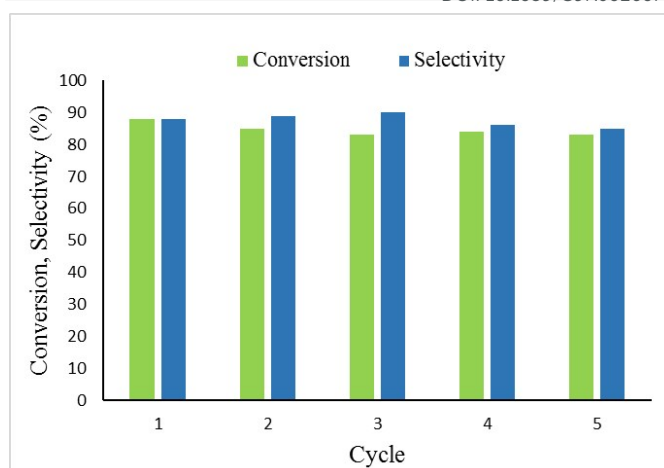


Fig. 7. Subsequent reaction cycles of Co-POM@MIL-101(3) in the cycloaddition of CO₂ with styrene epoxide, reaction conditions: 200 mg Co-POM@MIL-101(3), 15 mmol styrene epoxide, P_{CO2} = 20 bar, T = 90 °C, 2 h for each run.

After each run, the filtrated catalyst was washed with water and chloroform and activated under vacuum at 100 °C overnight. The Co-POM leaching for both reactions was determined by analyzing the collected filtrates using ICP. The results showed that only negligible amounts of Co-POM catalyst leached in both reactions (less than 1% after the last run). The nature of the reused catalyst after the last run was monitored by XRD (Fig. S8 in the ESI†) which illustrated no significant difference between the fresh and re-used catalyst.

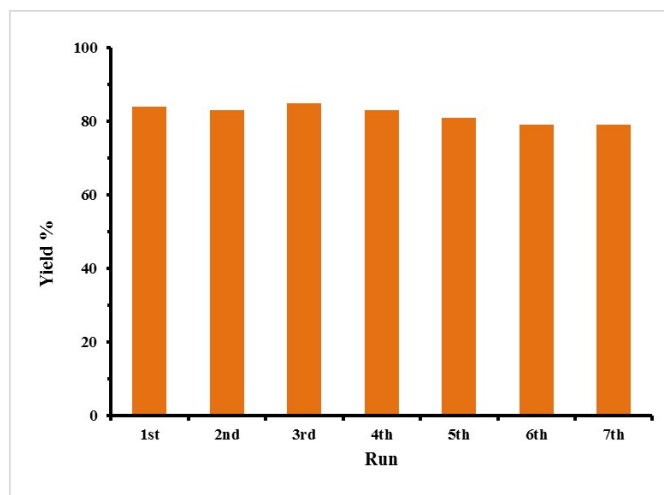
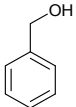
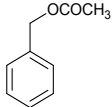
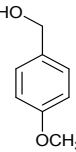
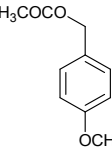
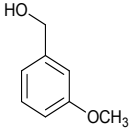
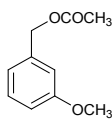
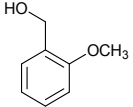
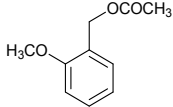
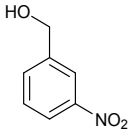
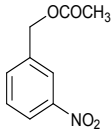
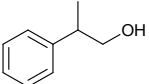
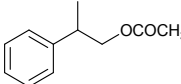
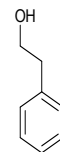
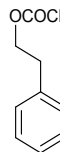


Fig. 8. Subsequent reaction cycles of Co-POM@MIL-101(3) in the esterification of acetic acid with benzyl alcohol, reaction conditions: 5 mmol acetic acid, 55 mmol alcohol, 100 mg catalyst, T = 70 °C, 25 min for each run.

ARTICLE

Table 7: Esterification of acetic acid with various alcohols catalyzed by Co-POM@MIL-101(3)^a

entry	alcohol	Ester	time (min)	yield (%) ^b	TOF ^c (h ⁻¹)
1			25	84	10500
2			25	100	12500
3			25	92	11500
4			40	100	7500
5			45	100	6700
6			25	100	12500
7			25	97	12100

^a Reaction conditions: 5 mmol acetic acid, 55 mmol alcohol, 100 mg catalyst, T = 70 °C. ^b GC yield based on acid. ^c (mol product/mol cobalt)h⁻¹.

Experimental Section

Materials and Instrumentation

All reagents were purchased as ACS reagent grade from Merck (Germany) or Fluka (Switzerland). Powder X-ray diffraction (PXRD) analysis was conducted using a D8 Advance instrument from Bruker (Germany) using Cu K α ($\lambda = 1.5406 \text{ \AA}$) radiation. N₂ adsorption-desorption isotherms at 77 K and CO₂ gas adsorption isotherms at 273 K were obtained on a Micromeritics Tristar instrument (France) equipped with a Smart VacPrep outgassing unit. The Brunauer-Emmett-Teller (BET) method and the Barrett, Joyner, and Halenda (BJH) method were used for calculation of the specific surface areas and the pore distribution, respectively. The chemical composition was determined using inductively coupled plasma

optical emission spectroscopy (ICP-OES), with a Jarrell-Ash 1100 ICP analyzer (Canada). X-ray photoelectron spectroscopy (XPS) was carried out using an ESCA M-Probe system from Surface Science Instruments equipped with a monochromatic Al K α excitation source ($\lambda = 8.33 \text{ \AA}$). Measurements were conducted at a pressure in the 10⁻⁹ mbar range. Survey scans were acquired with a detector pass energy of 158.9 eV, whereas high-resolution spectra were recorded with a pass energy of 22.9 eV. Spectral corrections and peak deconvolution were done with CasaXPS software (Casa Software Ltd.). Binding energies were charge-corrected in reference to the C 1s signal for adventitious carbon (284.8 eV). All spectra were fitted with Shirley or, where necessary, Spline Shirley backgrounds using a GL(30) line shape for non-conductive synthetic components and an asymmetric A(0.4, 0.38, 20)GL(20) line shape for C=C contributions. EPR spectra were recorded on solid samples in the X-band on a Bruker

(Germany) System ELEXSYS 500E equipped with a Bruker Variable Temperature Unit ER 4131VT (500 to 100 K); the g values were calibrated using a dpph sample. The progress of the reactions was monitored using GC analysis with an Agilent (USA) GC6890 equipped with a 19096C006 80/100 WHP packed column and a flame ionization detector. NH_3 and CO_2 temperature programmed desorption (TPD) experiments were carried out using a NanoSORD NS91 (Sensiran, Iran) apparatus.

Synthesis of the Co-POM@MIL-101 catalysts

Co-POM was synthesized according to the literature⁷² and the Co-POM@MIL-101 catalysts were prepared according to our previously reported procedure.¹⁴ Briefly, the catalyst was synthesized by adding the MIL-101(Cr) precursor, including $\text{Cr}(\text{NO}_3)_3 \cdot 9\text{H}_2\text{O}$ (2.0 g, 5 mmol), terephthalic acid (0.83 g, 5 mmol), and Co-POM (0.4 g (0.129 mmol), 0.8 g (0.258 mmol), 1.0 g (0.323 mmol), 2.0 g (0.645 mmol), and 2.5 g (0.806 mmol)) and deionized water (20 mL) in a Teflon-lined autoclave reactor. After sonicating for a short time, the mixture was put in the oven at 218 °C for 18 h without stirring. The resulting solid Co-POM@MIL-101 was filtered off by centrifugation and washed with water, ethanol, and acetone, followed by drying and activation at 100 °C under vacuum overnight.

General procedure for the cycloaddition of CO_2 with epoxides

The reactions were conducted in a 75 mL stainless steel autoclave equipped with a magnetic stirrer. For a typical catalytic reaction, catalyst (200 mg including 0.002 mmol of Co-POM, calculated based on Co), epoxide (15 mmol) and tetrabutylammonium bromide (1 mmol) were placed in the reactor. The autoclave was charged three times with CO_2 to deplete air, then pressurized with the appropriate amount of CO_2 and heated to the desired temperature in an oil bath for the designated period of time. After the reaction was complete, the autoclave was cooled to 0 °C in an ice-water bath, and the remaining CO_2 was slowly released. The product was diluted with ethyl acetate and the reaction yield was determined by GC analysis. The catalysts were separated via centrifugation, washed with ethyl acetate and DMF, dried under vacuum at 150 °C and then reused directly for the next run.

General procedure for the esterification reaction

Acetic acid and alcohol were introduced into a two-necked round bottom flask connected to a reflux condenser and a thermometer. The reaction mixture was heated using an oil bath at 70 °C and then the catalyst was added. To follow the

reaction, aliquots were periodically collected for GC analysis. Valeric acid was used as an internal standard and the yield of the reaction was reported based on the amount of acetic acid. The catalyst was separated via centrifugation prior to gas chromatography analysis. To avoid any additional conversion in the reaction mixture, the analysis was carried out directly after sampling. For the recycling tests, the catalyst Co-POM@MIL-101(3) was recovered by filtration, washed with water and chloroform, and dried under vacuum at 100 °C. The recovered catalyst was directly used for the next run.

Conclusions

The effect of the encapsulation of the Keggin anion $[\text{Co}(\text{III})\text{W}_{12}\text{O}_{40}]^{5-}$ (Co-POM) in the MOF MIL-101(Cr) on the catalytic activity of Co-POM@MIL-101 catalysts in the cycloaddition of CO_2 with epoxides, as well as in the esterification of acetic acid with alcohol was investigated in this study.

The thorough characterization of the catalyst materials revealed good encapsulation and distributions of the Co-POM in the MOF (SEM, TEM, EDX). The low Co content of less than 1% from EDX was confirmed by XPS alongside with an increased tendency of electron transfer from Cr(III) of MIL-101 to Co(III) with increasing Co-POM contents resulting in the observation of Cr(IV) and Co(II) in XPS and EPR spectra.

The facile Co(III)/Co(II) electron transfer seems to be important for the two studied reactions. For the cycloaddition of CO_2 with epoxides a Co(III)/Co(II) mediated reaction mechanism could be proposed based on the observation that the Lewis acid-base character of the components MIL-101(Cr) and Co-POM as determined from NH_3 and CO_2 temperature programmed desorption (TPD) experiments do not correlate with the observed catalytic efficiency. The same is true for the esterification of acetic acid and various alcohols. Trapping experiments using radical scavengers as acrylonitrile and 2,6-di-tert-butylphenol support strongly electron-transfer triggered mechanisms for both reactions.

The easy-to-make catalyst system Co-POM@MIL-101 allows to carry out these interesting reactions using a plethora of substrates, under solvent-free conditions, low conversion times, high TOF and selectivity, at low temperature and the catalyst can be easily recycled and has been reused several times. This success underlines that the encapsulation of POM catalysts in MOF or related porous materials is an interesting approach to design highly active, selective and easily recoverable catalysts.

ARTICLE

Table 8. Comparison of catalytic performance of Co-POM@MIL-101 and reported catalysts for esterification of acetic acid.

entry	catalyst	alcohol	T (°C)	time (h)	yield (%)	reusability (runs)	Ref
1	Co-POM/UiObpy ^a	1-propanol	60	7	30	2	11
2	HPW@MIL-101(Cr) ^b	n-hexanol	110	6	58.3	5	73
3	MIL-125s	butanol	90	7	75.2	3	45
4	poly(VMPS)-PW ^c	butanol	110	1.5	97.4	6	74
5	Fe(ClO ₄) ₃	benzyl alcohol	R.T	15	95	homogeneous	75
6	POM-IL ^d	benzyl alcohol	100	6	89.2	8	76
7	p-phenolsulfonic acid formaldehyde resins	benzyl alcohol	50	12	94	no data	77
8	Co-POM@MIL-101(3)	benzyl alcohol	70	25 min	84	7	present work

^a UiO-bpy: Zr-MOFs connected by 2,2'-bipyridine-5,5'-dicarboxylic acid linkers. ^b HPW = [PW₁₂O₄₀]³⁻ SO₃H functionalized [PW₁₂O₄₀]³⁻. ^c POM = [HPW₁₂O₄₀]²⁻.

Conflicts of interest

There are no conflicts to declare.

Acknowledgments

We are thankful to the Research Council of the University of Isfahan for financial support of this work. AK acknowledges the German Academic Exchange Service (DAAD), KD-0001052598-2 for a short-time guest lectureship and the University of Shiraz. AS, RF, AK, and SM kindly acknowledge support from the University of Cologne.

Notes and references

- R. M. Ladera, J. L. G. Fierro, M. Ojeda and S. Rojas, *J. Catal.*, 2014, **312**, 195–203.
- S. S. Balula, I. C. Santos, L. Cunha-Silva, A. P. Carvalho, J. Pires, C. Freire, J. A. Cavaleiro, B. de Castro and A. M. Cavaleiro, *Catal. Today*, 2013, **203**, 95–102.
- Y. Yang, Y. Guo, C. Hu, Y. Wang and E. Wang, *Appl. Catal. A: Gen.*, 2004, **273**, 201–210.
- O. Kholdeeva, N. Maksimchuk and G. Maksimov, *Catal. Today*, 2010, **157**, 107–113.
- R. R. Ozer and J. L. Ferry, *J. Phys. Chem. B*, 2002, **106**, 4336–4342.
- G. Ferey, *Science*, 2005, **310**, 1119–1119.
- N. Maksimchuk, M. Timofeeva, M. Melgunov, A. Shmakov, Y. A. Chesalov, D. Dybtsev, V. Fedin and O. Kholdeeva, *J. Catal.*, 2008, **257**, 315–323.
- J. Juan-Alcañiz, J. Gascon and F. Kapteijn, *J. Mater. Chem.*, 2012, **22**, 10102–10118.
- D.-Y. Du, J.-S. Qin, S.-L. Li, Z.-M. Su and Y.-Q. Lan, *Chem. Soc. Rev.*, 2014, **43**, 4615–4632.
- W. Xie and F. Wan, *Chem. Engin. J.* 2019, **365**, 40–50.
- X. Song, D. Hu, X. Yang, H. Zhang, W. Zhang, J. Li, M. Jia, and J. Yu, *ACS Sustainable Chem. Eng.* 2019, **7**, 3624–3631.
- M. Stuckart and K. Y. Monakhov, *J. Mater. Chem. A*, 2018, **6**, 17849–17853.
- N. V. Maksimchuk, O. A. Kholdeeva, K. A. Kovalenko, and V. P. Fedin, *Isr. J. Chem.* 2011, **51**, 281–289.
- A. Marandi, S. Tangestaninejad, M. Moghadam, V. Mirkhani, A. Mechler, I. Mohammadpoor-Baltork and F. Zadehahmadi, *Appl. Organomet. Chem.*, 2018, **32**, e4065
- C.-Y. Sun, S.-X. Liu, D.-D. Liang, K.-Z. Shao, Y.-H. Ren and Z.-M. Su, *J. Am. Chem. Soc.*, 2009, **131**, 1883–1888.
- L. H. Wee, S. R. Bajpe, N. Janssens, I. Hermans, K. Houthoofd, C. E. Kirschhock and J. A. Martens, *Chem. Commun.*, 2010, **46**, 8186–8188.
- L. H. Wee, N. Janssens, S. R. Bajpe, C. E. Kirschhock and J. A. Martens, *Catal. Today*, 2011, **171**, 275–280.
- B. Gagea, Y. Lorgouilloux, Y. Altintas, P. Jacobs and J. Martens, *J. Catal.*, 2009, **265**, 99–108.
- I. A. Weinstock, *Chem. Rev.*, 1998, **98**, 113–170.
- C. Saux, L. R. Pizzio, L. B. Pierella, *Appl. Catal. A: Gen.*, 2013, **452**, 17–23.

21. E. N. Glass, J. Fielden, Z. Huang, X. Xiang, D. G. Musaev, T. Lian and C. L. Hill, *Inorg. Chem.*, 2016, **55**, 4308–4319.
22. S. Mukhopadhyay, J. Debgupta, C. Singh, A. Kar and S. K. Das, *Angew. Chem., Int. Ed.*, 2018, **57**, 1918–1923.
23. J. Juan-Alcañiz, E. V. Ramos-Fernandez, U. Lafont, J. Gascon and F. Kapteijn, *J. Catal.*, 2010, **269**, 229–241.
24. L. Bromberg, Y. Diao, H. Wu, S. A. Speakman and T. A. Hatton, *Chem. Mater.*, 2012, **24**, 1664–1675.
25. G. Férey, C. Mellot-Draznieks, C. Serre, F. Millange, J. Dutour, S. Surlblé and I. Margiolaki, *Science*, 2005, **309**, 2040–2042.
26. M. North, R. Pasquale and C. Young, *Green Chem.*, 2010, **12**, 1514–1539.
27. M. M. Halmann, *Chemical Fixation of Carbon Dioxide – Methods for Recycling CO₂ into Useful Products*, CRC Press, Boca Raton, 2018.
28. Y. Leng, D. Lu, C. Zhang, P. Jiang, W. Zhang and J. Wang, *Chem. Eur. J.*, 2016, **22**, 8368–8375.
29. J. A. Kozak, J. Wu, X. Su, F. Simeon, T. A. Hatton and T. F. Jamison, *J. Am. Chem. Soc.*, 2013, **135**, 18497–18501.
30. Y. Wang, Y. Qin, X. Wang and F. Wang, *Catal. Sci. Technol.*, 2014, **4**, 3964–3972.
31. F. Liu, K. Huang, A. Zheng, F.-S. Xiao and S. Dai, *ACS Catal.*, 2018, **8**, 372–391.
32. K. Huang, J.-Y. Zhang, F. Liu and S. Dai, *ACS Catal.*, 2018, **8**, 9079–9102.
33. F. Liu, K. Huang, C.-J. Yoo, C. Okonkwo, D.-J. Tao, C. W. Jones and S. Dai, *Chem. Eng. J.*, 2017, **314**, 466–476.
34. F. Liu, K. Huang, Q. Wu and S. Dai, *Adv. Mater.*, 2017, **29**, 1700445 (1–8).
35. K. Huang, F. Liu and S. Dai, *J. Mater. Chem. A*, 2016, **4**, 13063–13070.
36. F. Liu, K. Huang, S. Ding and S. Dai, *J. Mater. Chem. A*, 2016, **4**, 14567–14571.
37. W. Ge, X. Wang, L. Zhang, L. Du, Y. Zhou and J. Wang, *Catal. Sci. Technol.*, 2016, **6**, 460–467.
38. F. Chen, X. Li, B. Wang, T. Xu, S. L. Chen, P. Liu and C. Hu, *Chem. Eur. J.*, 2012, **18**, 9870–9876.
39. Q. Han, B. Qi, W. Ren, C. He, J. Niu and C. Duan, *Nat. Commun.*, 2015, **6**, 10007 (1–8).
40. Y.-B. Huang, J. Liang, X.-S. Wang and R. Cao, *Chem. Soc. Rev.*, 2017, **46**, 126–157.
41. T. S. Reddy, M. Narasimhulu, N. Suryakiran, K. C. Mahesh, K. Ashalatha and Y. Venkateswarlu, *Tetrahedron Lett.*, 2006, **47**, 6825–6829.
42. N. G. Khaligh, *J. Mol. Catal. A: Chemical*, 2012, **363**, 90–100.
43. G. Bartoli, M. Bosco, R. Dalpozzo, E. Marcantoni, M. Massaccesi and L. Sambri, *Eur. J. Org. Chem.*, 2003, **2003**, 4611–4617.
44. M. Popova, H. Lazarova, Y. Kalvachev, T. Todorova, Á. Szegedi, P. Shestakova, G. Mali, V. D. Dasireddy and B. Likozar, *Catal. Commun.*, 2017, **100**, 10–14.
45. E. Yilmaz, E. Sert and F. S. Atalay, *Catal. Commun.*, 2017, **100**, 48–51.
46. Q.-X. Luo, M. Ji, M.-H. Lu, C. Hao, J.-S. Qiu and Y.-Q. Li, *J. Mater. Chem. A*, 2013, **1**, 6530–6534.
47. B. Babu, Ch. R. Krishna, Ch. V. Reddy, V. P. Manjari and R. V. S. S. N. Ravikumar, *Spectrochim. Acta A: Molecular and Biomolecular Spectroscopy*, 2013, **109**, 90–96.
48. K. Ravindranadh, K. D. V. Prasad and M. C. Rao, *AIMS Mater. Sci.* 2016, **3**, 796–807.
49. W. E. Antholine, S. Zhang, J. Gonzales and N. Newman, *Int. J. Mol. Sci.* 2018, **19**, 3532 (1–7).
50. A. G. Shard, *Surf. Interface Anal.*, 2014, **46**, 175–185.
51. M. C. Biesinger, B. P. Payne, A. P. Grosvenor, L. W. M. Lau, A. R. Gerson, R. St. C. Smart, *Appl. Surf. Sci.*, 2011, **257**, 2717–2730.
52. T. H. Fleisch, G. W. Zajac, J. O. Schreiner and G. J. Mains, *Appl. Surf. Sci.*, 1986, **26**, 488–497.
53. Y. Xie, Z. Fang, L. Li, H. Yang and T.-F. Liu, *ACS Appl. Mater. Interfac.*, 2019, **11**, 27017–27023.
54. F. Soltanolkotabi, M. R. Talaie, S. Aghamiri and S. Tangestaninejad, *J. Iran. Chem. Soc.*, 2019 published online, <https://doi.org/10.1007/s13738-019-01746-8>.
55. J. Graciani, K. Mudiyansele, F. Xu, A. E. Baber, J. Evans, S. D. Senanayake, D. J. Stacchiola, P. Liu, J. Hrbek, J. Fernández Sanz and J. A. Rodriguez, *Science*, 2014, **345**, 546–550.
56. A. K. Opitz, A. Nennung, C. Rameshan, M. Kubicek, T. Götsch, R. Blume, M. Hävecker, A. Knop-Gericke, G. Rupprechter, B. Klötzer and J. Fleig, *ACS Appl. Mater. Interfaces*, 2017, **9**, 35847–35860.
57. J. Kim, S.-N. Kim, H.-G. Jang, G. Seo and W.-S. Ahn, *Appl. Catal. A: General*, 2013, **453**, 175–180.
58. K. Kamata and K. Sugahara, *Catalysts*, 2017, **7**, 345 (1–24).
59. L. Zhu, X.-Q. Liu, H.-L. Jiang and L.-B. Sun, *Chem. Rev.*, 2017, **117**, 8129–8176.
60. M. North and R. Pasquale, *Angew. Chem.*, 2009, **121**, 2990–2992.
61. S.-S. Wu, X.-W. Zhang, W.-L. Dai, S.-F. Yin, W.-S. Li, Y.-Q. Ren and C.-T. Au, *Appl. Catal. A: Gen.*, 2008, **341**, 106–111.
62. L.-F. Xiao, F.-W. Li, J.-J. Peng and C.-G. Xia, *J. Mol. Catal. A: Chemical*, 2006, **253**, 265–269.
63. J. Sun, L. Han, W. Cheng, J. Wang, X. Zhang and S. Zhang, *ChemSusChem*, 2011, **4**, 502–507.
64. O. V. Zalomaeva, A. M. Chibiryaev, K. A. Kovalenko, O. A. Kholdeeva, B. S. Balzhinimaev and V. P. Fedin, *J. Catal.*, 2013, **298**, 179–185.
65. R. Babu, A. C. Kathalikkattil, R. Roshan, J. Tharun, D.-W. Kim and D.-W. Park, *Green Chem.*, 2016, **18**, 232–242.
66. B. Yu, B. Zou and C.-W. Hu, *J. CO₂ Util.*, 2018, **26**, 314–322.
67. M.-Y. Wang, R. Ma and L.-N. He, *Sci. China: Chem.*, 2016, **59**, 507–516.
68. X.-B. Lu and D. J. Darensbourg, *Chem. Soc. Rev.*, 2012, **41**, 1462–1484.
69. J. Zhao, H. Guan, W. Shi, M. Cheng, X. Wang and S. Li, *Catal. Commun.*, 2012, **20**, 103–106.
70. B. Yu, B. Zou and C.-W. Hu, *J. CO₂ Util.*, 2018, **26**, 314–322.
71. Y. Cao, Q. Chen, C. Shen and L. He, *Molecules* 2019, **24**, 2069 (1–26).
72. M. H. Habibi, S. Tangestaninejad, I. Mohammadpoor-Baltork, V. Mirkhani and B. Yadollahi, *Tetrahedron Lett.*, 2001, **42**, 6771–6774.
73. Y. Zang, J. Shi, X. Zhao, L. Kong, F. Zhang and Y. Zhong, *React. Kinet. Mech. Catal.*, 2013, **109**, 77–89.
74. Y. Leng, P. Jiang and J. Wang, *Catal. Commun.*, 2012, **25**, 41–44.
75. M. M. Heravi, F. K. Behbahani, R. H. Shoar and H. A. Oskooie, *Catal. Commun.*, 2006, **7**, 136–139.
76. H. Li, Y. Qiao, L. Hua, Z. Hou, B. Feng, Z. Pan, Y. Hu, X. Wang, X. Zhao and Y. Yu, *ChemCatChem*, 2010, **2**, 1165–1170.
77. M. Minakawa, H. Baek, Y. M. Yamada, J. W. Han and Y. Uozumi, *Org. Lett.*, 2013, **15**, 5798–5801.

Graphical Abstract

